Simulating Collisional Dark Matter

Javier Alejandro Acevedo Barroso

November 4, 2018

Contents

List of Figures

0.1 General Objetive

To simulate the phase space of a collisional dark matter fluid using a Lattice-Boltzmann method.

0.2 Specific Objetives

- To implement a Lattice-Boltzmann simulation using a 4-dimensional phase space and a varying collisional term.
- To implement a Lattice-Boltzmann simulation using a 6-dimensional phase space and a varying collisional term.
- To study the dynamical behavior of a dark matter fluid using different equilibrium distributions in the collisional term.
- To simulate the phase space of a collisional dark matter fluid using literature values for the thermally averaged cross-section and compare it with its collisionless version.

Chapter 1

Introduction

In this work we simulate the phase space of a collisional dark matter fluid using a Lattice-Boltzmann simulation. Traditionally, dark matter has been simulated by using N-body schemes, in which the temporal evolution of a system of N particles is simulated usually by solving the Poisson-Vlasov equation[1]. These N-body simulations have been essential for modern cosmology and the characterization of the dark matter halos. For example, the acceptance of the ΛCMD cosmology began with an N-body simulation of the large-scale structure of the universe, using only 32748 particles!.[2] In order to follow the ideas and developments of the upcoming chapters, it is essential to understand some concepts and computational techniques. In this chapter, we present all the necessary knowledge for the proper understanding of this work.

1.1 General Objetive

To simulate the phase space of a collisional dark matter fluid using a Lattice-Boltzmann method.

1.2 Specific Objetives

- To implement a Lattice-Boltzmann simulation using a 4-dimensional phase space and a varying collisional term.
- To implement a Lattice-Boltzmann simulation using a 6-dimensional phase space and a varying collisional term.
- To study the dynamical behavior of a dark matter fluid using different equilibrium distributions in the collisional term.
- To simulate the phase space of a collisional dark matter fluid using literature values for the thermally averaged cross-section and compare it with its collisionless version.

1.3 Dark Matter

Modern cosmology describes the universe as being composed of two fundamental types of energy: dark energy and matter[1], with dark energy being associate with

[1] In relativity, mass and energy are equivalent.

a cosmological constant and matter being divided into two categories: dark matter and standard model matter[2]. The energy density of the universe is 69% dark energy and 31% matter.

Standard model matter includes all the particles whose interactions can be properly described by the standard model, such as: Protons, Electrons, Atoms and naturally, any structure that they form, like Humans or Stars. On the other hand, dark matter is all the matter we measure from astrophysical sources which cannot be explained by baryonic matter. We know of the existence of dark matter entirely from astrophysical evidence, during this section we are going to do an historical review of such evidence.

1.3.1 The Cluster Missing Mass Problem

The traditional history of dark matter begins in the 1930s with the swiss astronomer Fritz Zwicky[3] [4], who noticed an unusually high velocity dispersion between the galaxies of the Coma Cluster. To tackle the problem, Zwicky assumed that the Coma Cluster "had already reached a mechanically stationary state" [5] and such, the virial theorem could be applied. By counting galaxies, along with assuming that matter is distributed uniformly in the cluster and using Hubble's estimate of the mean mass of a galaxy, Zwicky was able to estimate the potential energy of the Cluster. Using his estimate of the visible mass and the virial theorem, Zwicky concluded that the velocity dispersion must be $\sqrt{\bar{v^2}} = 80$ km/s. Nonetheless, the real measurement of the velocity dispersion was $\sqrt{\bar{v^2}} = 1000$ km/s, implying a virial mass about 400 times larger than the visible mass[3]. Zwicky called the discrepancy between the luminous

[2]Which is very often called "Baryonic matter" due to Baryions being the largest fraction of this mass.

[3]This ratio is often called the mass-to-light ratio.

matter (in the form of visible galaxies which could simply be counted) and the virial matter (obtained from the virial theorem and the high velocity dispersion of the cluster) "Dark Matter".

By the late 1950s similar calculations for different clusters had been published. Many of those calculations had very large values for the mass-to-light ratio[6], which were consistent with the mass-to-light ratio calculated from the Coma Cluster. The problem of the missing mass seemed to appear in almost every large scale structure in the universe, and by the early 1970s astrophysicist had already disregarded hot gas[7] and free hydrogen[8] as explanations for the missing mass in Clusters. Nonetheless, it was still possible that the missing mass problem could be in fact solved by a more refined model of the cluster kinematics, because so far, the missing mass problem had only been observed on Clusters and large scale structures.

1.3.2 Galaxy Rotation Curves

A galaxy rotation curve plots the orbital velocity of stars in a galaxy versus their distance to the galaxy centre. These curves became important thanks to the work of the Indian astrophysics Subrahmanyan Chandrasekhar, who proved that the mutual interactions of stars were negligible, so a galaxy could be modeled as a non-interacting system of stars. Such modeling allows to obtain mass profiles from galaxy rotation curves. Now, due to photometric measurements, astrophysicist believed that most of the mass was overwhelmingly concentrated in the galaxy centre, therefore, it was reasonable to model the galaxy similarly to the solar system.

Consider a star in the galaxy disk with mass m at a distance r from the galaxy

centre. Given that we can disregard the interaction between starts, the sum of forces acting on the object is simply the gravitational attraction towards the galaxy centre:

$$m\frac{v^2}{r} = G\frac{mM}{r^2} \tag{1.1}$$

With M being the mass enclosed by the star orbit and v being the orbital velocity of the star. Finally, the galaxy rotation curve for such galaxy will be given by:

$$v(r) = \sqrt{\frac{GM}{r}} \tag{1.2}$$

Which means that for objects outside of the galaxy disk (but still under the influence of the galaxy gravitational pull), the enclosed mass will be constant regardless of the radius, and thus, the orbital velocity will be proportional to $r^{-1/2}$. With the advent of radio astronomy and the invention of the Image Tube Spectrograph, astronomers were able to measure orbital velocities way beyond the apparent end of the luminous galaxy disks, only to find that the orbital velocity did not decay proportionally to $r^{-1/2}$ but it stayed more or less constant[9] [10] [11]. This behavior can be seen more easily in the figure 1.1:

This unexpected velocity profile implied a mass-to-light ratio that increased with distance and the existence of mass beyond the visible galactic disk[12]. The overwhelming amount of high quality galaxy rotation curves measurements, let to the acceptance of the dark matter hypothesis in the astrophysical community.

Throughout the use of numerical simulations and the measurement of more galaxy rotation curves during the 1980s and the 1990s, it was concluded that the dark matter density in galaxies was well modeled by the Navarro-Frenk-White (NFW)

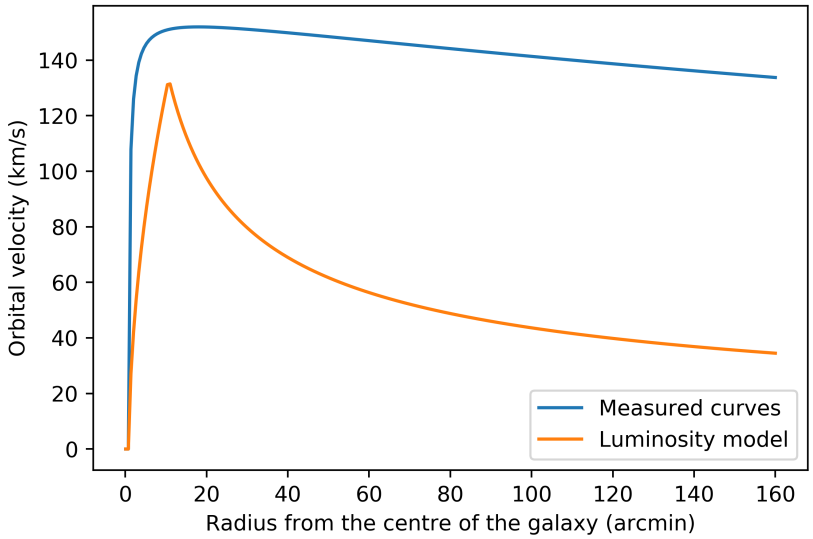

Figure 1.1: A comparison between the model from photometrical measurements and the curves measured. This curves are illustrative and do not correspond to a particular galaxy.

profile[13][14]

$$\rho(r) = \frac{\rho_0}{r/r_s(1 + r/r_s)^2} \tag{1.3}$$

1.3.3 The Bullet Cluster

Galaxy clusters have three main constituents: dark matter, intracluster gas (which is mostly ionised hydrogen and helium), and the galaxy themselves.[15]

We can observe the intracluster baryonic matter in the x-ray band thanks to Bremsstrahlung radiation, therefore, by doing photometry to x-ray pictures it is possible to map the baryonic gas distribution in a cluster. In the case of dark matter, we infer its existence in clusters thanks to the work of Fritz Zwicky and the posterior work in the

missing mass problem in galaxy clusters. Our current estimates place most of the cluster mass in the dark matter component. By analyzing the gravitational lensing effect (in particular the *weak* gravitational lensing effect), it is possible to map the mass distribution in a galaxy cluster. Given that most of the cluster mass is dark matter, weak lensing mapping ends up creating a map of the dark matter distribution in a galaxy cluster. Lastly, we can observe the galaxies in the visual and the infrared band. They are the only component of a galaxy cluster that can be observed in the visual band. About 90 percent of the mass of a cluster is dark matter (this is not a surprise since Fritz Zwicky measured mass-to-light ratios of 50 during the 1930s). Of the remaining baryonic matter, the ionized gas mass can represent up to 90% of the mass, making galaxies responsable of about 1% of the cluster mass. The object

Bullet Cluster (also known as 1E 0657-558) is the aftermath of the collision of two galaxy cluster. Before the collision, each cluster had its own galaxies, baryonic gas and dark matter, and the center of mass of each constituent coincided with the center of mass of the whole cluster. During the collision, each constituent reacts differently to the situation. Galaxies, given that the occupy a minuscule volume in the cluster, are essentially collisionless. Two galaxy clusters can collide without any galaxy (or very little galaxies) colliding per se.

1.4 Types of Dark Matter

1.5 The Boltzmann Equation

1.6 Lattice Automata and Lattice Boltzmann

1.7 BGK Approximation

Chapter 2

The Lattice Boltzmann Algorithm

2.1 General Description

Now that we have overviewed the pertinent concepts, we can proceed to the particulars of this implementation. As previously asserted, the heart of the Lattice-Boltzmann Algorithm lies on its discretization of the phase space[16] [17].

To discretize the phase space, we must choose the region to simulate. In this work, we name the extremal values in the w axis of the phase space W_{min} and W_{max}. Then, one has to fix either the size of the grid or the size of the lattice. We name the size of the grid in the w axis N_w (i.e. N_x or N_{vz}). The size of the lattice in the w axis (which we are going to name dw) and the extremal values are related by:

$$dw = \frac{W_{max} - W_{min}}{N_w} \tag{2.1}$$

In this work we are going to use the phase-space mass density, which means that $f(\mathbf{r}, \mathbf{v}, t)\mathrm{d}\mathbf{r}\mathrm{d}\mathbf{v}$ is the density of dark matter whose position is between $\mathbf{r}$ and $\mathbf{r} + \mathrm{d}\mathbf{r}$, and its velocity is between $\mathbf{v}$ and $\mathbf{v} + \mathrm{d}\mathbf{v}$. Now that we have properly defined the phase space grid, we can proceed to initialization. For simplicity, we choose gaussian initial conditions given by:

$$f(\mathbf{r}, \mathbf{v}, 0) = A \exp\left\{ -\frac{\mathbf{r}^2}{\sigma_r^2} - \frac{\mathbf{v}^2}{\sigma_v^2} \right\} \tag{2.2}$$

Where $f(\mathbf{r}, \mathbf{v}, 0)$ is the initialization of the phase space density, A is an indirect measure of the total mass in the system, $\mathbf{r}$ is the vector (x, y, z), $\mathbf{v}$ is the vector (vx, vy, vz), and σ_i are a measure of the width of the gaussian profile in the given axis. Note that we use a single width for the spatial axis ($\sigma_{\mathbf{r}}$) and a single width for the velocity axis ($\sigma_{\mathbf{r}}$).

After initialization, the system evolves by the action of the Louville operator and the Collisional operator, nonetheless, the collisions are modeled as instant, which allows to concentrate they entire influence in a collisional step. The schematics of the algorithm can be seen easily in figure 2.1.

Now that we have defined the phase-space, we can obtain the spatial density of matter by integrating the phase space:

$$\rho(\mathbf{r}, t) = \int_{-\infty}^{\infty} f(\mathbf{r}, \mathbf{v}, t)\, \mathrm{d}\mathbf{v}. \tag{2.3}$$

When evaluating in the lattice the integral becomes a sum over the entire velocity lattice:

$$\rho(\mathbf{r}, t) = \sum_{\mathbf{v}_{min}}^{\mathbf{v}_{max}} f(\mathbf{r}, \mathbf{v}, t)\, \mathrm{d}\mathbf{v} \tag{2.4}$$

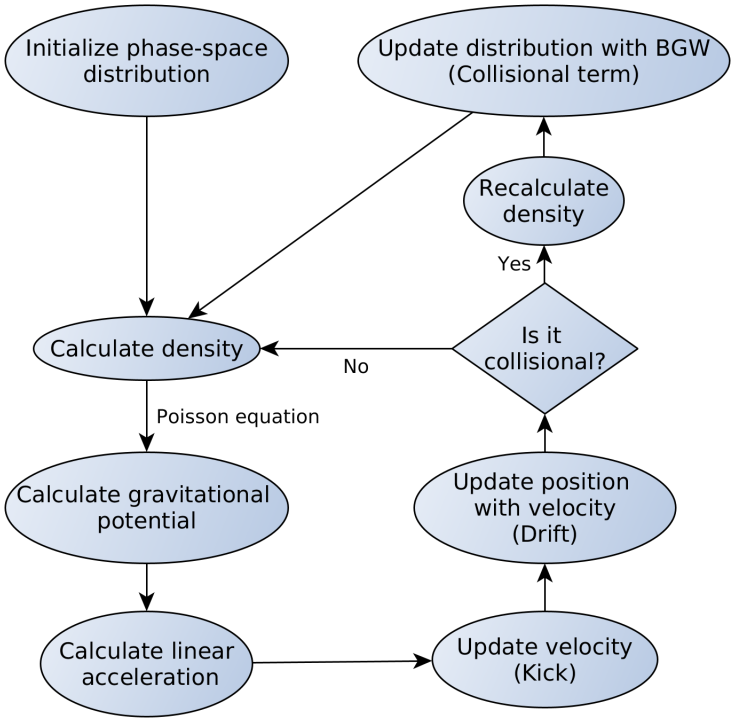

Figure 2.1: Flowchat of the algorithm.

and during initialization:

$$\rho(\mathbf{r}, 0) = \sum_{\mathbf{V}_{min}}^{\mathbf{V}_{max}} f(\mathbf{r}, \mathbf{v}, 0)\, \mathrm{d}\mathbf{v} \tag{2.5}$$

Once we have calculated the density, we solve the Poisson equation to obtain the potential due to gravitational interaction: [17]

$$\nabla^2 \Phi(\mathbf{r}, t) = 4\pi G \rho(\mathbf{r}, t) \tag{2.6}$$

Where $\Phi(\mathbf{r}, t)$ is the gravitational potential and G is the gravitational constant. To solve the Poisson equation we use the Fourier pseudo-spectral method, which

allows for very fast numerical solutions by making use of the Fast Fourier Transform algorithm. The idea is simply to apply a Fast Fourier Transform (FFT) to the density, then solve the equation in the Fourier space, and then apply an inverse transform (IFFT). In the Fourier space the Poisson equation is given by[18] [19]

$$\lambda_{\mathbf{k}}^2 \hat{\Phi}(\mathbf{k}, t) = 4\pi G \hat{\rho}(\mathbf{k}, t) \tag{2.7}$$

Where $\hat{g}(\mathbf{k}, t)$ is the Fourier transform of $g(\mathbf{r}, t)$, and $\lambda_{\mathbf{k}}$ is a constant that depends on the size of the lattice and the wavevector $\mathbf{k}$. $\lambda_{\mathbf{k}}$ is calculated according to the approximation scheme used to solve the equation. In the the pseudo-spectral approximation, $\lambda_{\mathbf{k}}$ is given by:

$$\lambda_{\mathbf{k}}^2 = \left(\frac{2\pi k_x}{X_{max} - X_{min}}\right)^2 + \left(\frac{2\pi k_y}{Y_{max} - Y_{min}}\right)^2 + \left(\frac{2\pi k_z}{Z_{max} - Z_{min}}\right)^2 \tag{2.8}$$

Therefore, solving the Poisson equation in the Fourier space is reduced to simple arithmetic. Thanks to the highly efficient implementations of the Fast Fourier Transform Algorithm available nowadays, solving the Poisson equation takes very little time and computational resources. In this work we use the Fastest Fourier Transform of the West[20] subroutine to handle the Fast Fourier Transforms.

Once we have calculated potential, obtaining the acceleration is straight-forward:

$$\mathbf{a}(\mathbf{r}, t) = -\boldsymbol{\nabla} \Phi(\mathbf{r}, t) \tag{2.9}$$

Which, in the context of the lattice can be easily calculated with a central difference numerical derivative.

Now, in order to update the phase space, we must first define the time interval to

simulate: we name N_t the number of time *instants* to simulate and $\mathrm{d}t$ the length of each of such instants. After calculating the acceleration and defining $\mathrm{d}t$, we can update our phase space. The subtlety here is that we will only use integer arithmetic, which means that we do not exactly care about the change in velocity during a time $\mathrm{d}t$ but for how many cells in the phase space lattice that change represents. This is modeled by:

$$\mathbf{v}_{n+1} = \mathbf{v}_n + \lfloor \mathbf{a}_n \mathrm{d}t \rceil \tag{2.10}$$

With $\lfloor x \rceil$ representing the operator "to nearest integer", so that $\mathbf{v}$ and $\lfloor \mathbf{a}\mathrm{d}t \rceil$ are vectors of integers and n represents the time instant. The update of the velocity is known as "kick". Analogously, the update of the position is known as "drift", and is given by:

$$\mathbf{r}_{n+1} = \mathbf{r}_n + \lfloor \mathbf{v}_n \mathrm{d}t \rceil \tag{2.11}$$

The use of only integer arithmetics allows for the elimination of the rounding error but introduces lattice noise. Regardless, this method creates a one to one map with the continous solution.[16] [17]

The "kick" and "drift" together are known as the "Streaming" step, and it represents the classical movement of particles under a potential but without considering the collision of particles. If we want a collisionless simulation, we can just calculate again the density and continue the algorithm from there. If we want a collisional simulation, we must define a collisional step.

2.2 The Collisional Step

As previously mentioned, solving the collisional integral $C[f]$ is not straight-forward, as it depends on the modeling of the short range interactions that we decide to assign to the dark matter particle. Given that the short range interaction of dark matter is unknown, we avoid using an specific description of the microscopic interactions and choose to use a mesoscopic approach instead, as discussed in section 1.7. The BGK collisional operator is given by:

$$C[f] = -\frac{1}{\tau}(f(\mathbf{r}, \mathbf{v}, t) - f_e(\mathbf{r}, \mathbf{v})) \tag{2.12}$$

Which in the context of the direct integration scheme used in the simulation becomes:

$$f(\mathbf{r} + \mathbf{v}\mathrm{d}t, \mathbf{v}, t) = f(\mathbf{r}, \mathbf{v}, t) - \frac{\mathrm{d}t}{\tau}(f(\mathbf{r}, \mathbf{v}, t) - f_e(\mathbf{r}, \mathbf{v})) \tag{2.13}$$

The idea behind this approach is to recover the macroscopic description of the fluid without committing to a particular microscopic description. In this scenario, the macroscopic effects of the collisions is a local relaxation towards equilibrium, which the BKG operator models using a relaxation time τ and a local equilibrium distribution $f_e(\mathbf{r}, \mathbf{v})$.

In order to implement a collisional operator we add a collisional step after the streaming step, in which the system performs a relaxation with characteristic (relaxation) time τ towards the local equilibrium distribution $f_e(\mathbf{r}, \mathbf{v})$. It is important to notice that the BGK collisional operator is a *scattering* operator and does not consider annihilation or creation of particles.

After defining the collisional term, we have to choose a distribution fuction $f_e(\mathbf{r}, \mathbf{v})$. We claim that the phase space distribution relaxes towards equilibrum, which means a displacement in the phase space and not the introduction or annihilation of mass. Therefore, the equilibrium distribution must be perfectly *normalized* in order to enforce particle number conservation. We normalize this equilibrium distribution by using macroscopic quantities obtained by integrating the velocity part of the phase space. This macroscopic quantities are: the volumetric density $\rho(\mathbf{r}, t)$, the macroscopic velocity $\mathbf{u}(\mathbf{r}, \mathbf{v})$ and the internal energy $e(\mathbf{r}, \mathbf{v})$.

The volumetric density is the same density we have been using so far defined by the integral of equation 2.3. The macroscopic velocity $\mathbf{u}(\mathbf{r}, \mathbf{v})$ is defined by the integral:

$$\mathbf{u}(\mathbf{r}, \mathbf{v}) = \int_{-\infty}^{\infty} f(\mathbf{r}, \mathbf{v}, t)\, \mathbf{v} \mathrm{d}\mathbf{v}. \tag{2.14}$$

When evaluating in the lattice the integral becomes:

$$\mathbf{u} = \sum_{\mathbf{V}_{min}}^{\mathbf{V}_{max}} f(\mathbf{r}, \mathbf{v}, t)\, \mathbf{v} \mathrm{d}\mathbf{v} \tag{2.15}$$

And the internal energy is defined by the integral:

$$e(\mathbf{r}, \mathbf{v}) = \frac{1}{2} \int_{-\infty}^{\infty} f(\mathbf{r}, \mathbf{v}, t)\, (\mathbf{v} - \mathbf{u})^2 \mathrm{d}\mathbf{v}. \tag{2.16}$$

Which also becomes a sum when evaluating in the lattice:

$$e(\mathbf{r}, \mathbf{v}) = \frac{1}{2} \sum_{\mathbf{V}_{min}}^{\mathbf{V}_{max}} f(\mathbf{r}, \mathbf{v}, t)\, (\mathbf{v} - \mathbf{u})^2 \mathrm{d}\mathbf{v} \tag{2.17}$$

Note that we are not including explicitly the mass of the dark matter particle in this integrals because it has already been included in the phase space definition.

Now that we have well defined macroscopic variables, we can proceed to choose an equilibrium distribution. Such distribution must obey the next condition:

$$C[f_e] = 0 \tag{2.18}$$

Which simply means that if the system is already in local equilibrium, then there is no relaxation. This condition can also be stated as "the equilibrium function must be a collisional invariant". In order for $f_e(\mathbf{r}, \mathbf{v})$ to be a collisional invariant, it must be build with variables that are also collisional invariant. Fortunately, the macroscopic variables already defined in this chapter are also collisional invariants, and so, we can use them to build equilibrium distributions. The idea behind normalization is to obtain the same macroscopical variables when integrating over $f_e(\mathbf{r}, \mathbf{v})$ instead of $f(\mathbf{r}, \mathbf{v}, t)$ In this work we use distributions based on the Maxwellian velocity distribution.

First, we use the classical Maxwellian distribution with proper normalization:

$$f_e(\mathbf{r}, \mathbf{v}) = \frac{\rho}{[2\pi\ e(\mathbf{r}, \mathbf{v})]^{D/2}} \exp\left[-\frac{(\mathbf{v} - \mathbf{u})^2}{2\ e(\mathbf{r}, \mathbf{v})}\right] \tag{2.19}$$

Where D is the number of components in the vector $f(\mathbf{r}, \mathbf{v}, t)$. For example, if the system is a three dimensional dark matter halo, then D will be equal to three. The Maxwell distribution was originally used to describe the probability distribution of the velocity in gas under kinetic theory assumptions. Here, we assume collisions as a phenomena that happens instantly, and during the time in between, the mechanics

of the system is governed by the self-gravitational potential. Therefore, the Maxwell distribution is a good starting point for the collisional distribution.

The second equilibrium distribution we are going to use is

2.2.1 Units and systems to simulate

Throughout the development of the simulation we used two set of units-system to simulate. A Gaussian system with dimensions similars to those of the Milky Way, and a Gaussian system with dimensions similar to those of the Coma Cluster

To a set the units, we fix the value of one spatial unit (us), one unit of time (ut), and one unit of mass (um), and from there, we proceed to calculate the values of the physical constants in our units.

For the Milky Way's Gaussian distribution we chose:

$$1\ us = 20\ \text{kpc} \tag{2.20}$$

$$1\ ut = 0.003\ \text{t}_0 \tag{2.21}$$

$$1\ um = 10^{11}\ \text{M}_\odot \tag{2.22}$$

And for the Coma Cluster's Gaussian distribution we chose:

$$1\ us = satan0 \tag{2.23}$$

$$1\ ut = satan1 \tag{2.24}$$

$$1\ um = satan2 \tag{2.25}$$

Chapter 3

Results

For the development of this work we wrote and ran three simulations: a two dimensional phase space simulation (one spatial and one velocity dimension), a four dimensional phase space simulation, and a six dimensional phase space simulation. The first one was develop in order to reproduce the results of Philip Mocz and Sauro Succi published in 2016 [17], and the results of Sebastian Franco published in 2017 [16]. In addition to reproducing results, we also extended the simulation to account for a collisional operator and tested some equilibrium distributions. The four dimensional simulation was develop as a step to develop the six dimensional simulation. Developing a four dimensional simulation allows to implement and test the specifics of increasing dimensionality without much of the visualization problems that arise in a six dimensional simulation.

3.1 The two dimensional phase space

For the two dimensional simulation we only need two axis, which allows for a very high resolution simulation. We used an squared grid characterized by:

$$W_{min} = -1 \text{ us} \tag{3.1}$$

$$W_{max} = 1 \text{ us} \tag{3.2}$$

$$N_w = 2048 \tag{3.3}$$

$$dw = 1/1024 \text{ us} \tag{3.4}$$

We always use grid sizes of the form $N_w = 2^n$ because the Fast Fourier Transform algorithm performs better and faster when calculating discrete transforms of size $2^n\ 3^m\ 5^l$ for n,m,l positive integers.

The initialization of the phase space can be seen in figure 3.1, along with its correspondent spatial density. The Gaussian nature of both the phase space and the density can be appreciated. After initialization we proceed to calculate the potential and the acceleration, which can be seen in figure 3.2. The values used to initialize the phase space were:

$$\sigma_r = 0.2 \tag{3.5}$$

$$\sigma_r = 0.2 \tag{3.6}$$

$$A = 50 \text{ um} \tag{3.7}$$

$$\tag{3.8}$$

Which yields a total mass of 1.26×10^{12} $M_{\odot}$, a very similar value with recent estimates of the total mass of our galaxy's dark matter halo. [21]

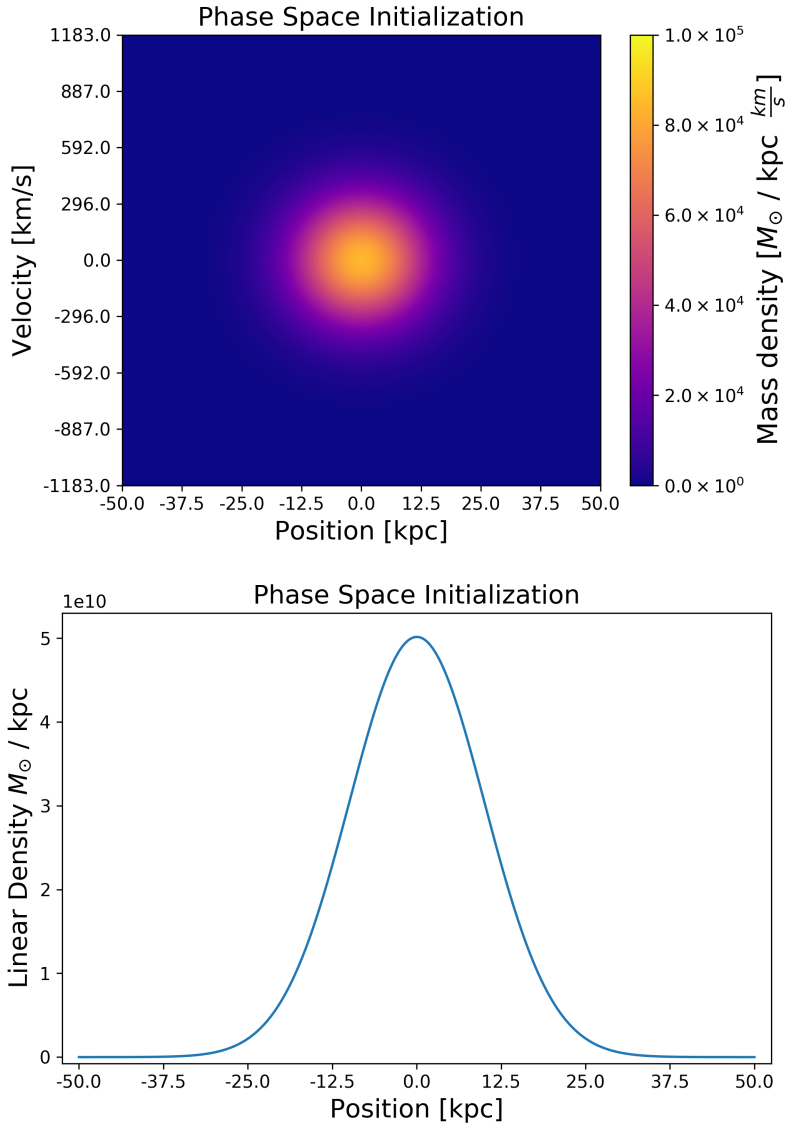

Figure 3.1: Up: initialization of the phase space. Down: the spatial density obtained through integration.

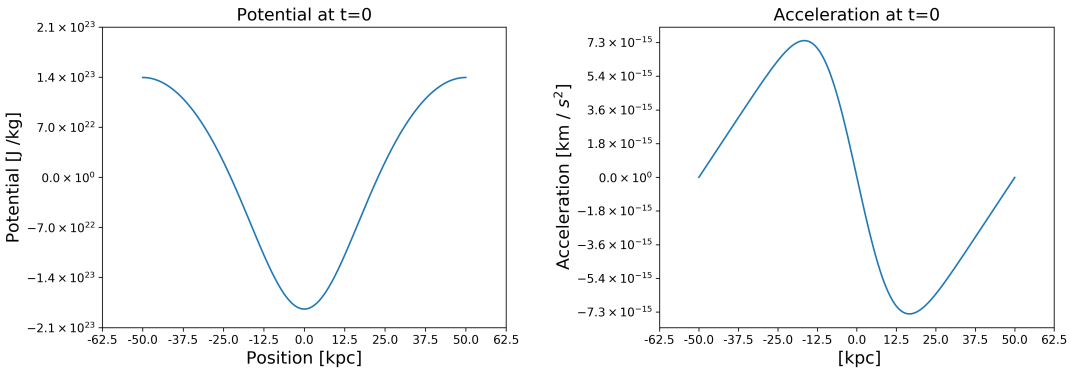

Figure 3.2: Left: The potential obtained by solving the Poisson equation. Right: The acceleration obtain by numerical derivation of the potential.

3.2 No collisional

3.3 Collisional with reported $< \sigma v >$

3.4 Different equlibrium distributions

Chapter 4

Conclusions

4.1 A Numerically Stable Simulation

Bibliography

[1] M. Kuhlen, M. Vogelsberger, and R. Angulo. Numerical simulations of the dark universe: State of the art and the next decade. *Physics of the Dark Universe*, 1:50–93, November 2012.

[2] M. Davis, G. Efstathiou, C. S. Frenk, and S. D. M. White. The evolution of large-scale structure in a universe dominated by cold dark matter. , 292:371–394, May 1985.

[3] Gianfranco Bertone and Dan Hooper. A History of Dark Matter. *Submitted to: Rev. Mod. Phys.*, 2016.

[4] J. M. Cline. TASI Lectures on Early Universe Cosmology: Inflation, Baryogenesis and Dark Matter. *ArXiv e-prints*, July 2018.

[5] H. Andernach and F. Zwicky. English and Spanish Translation of Zwicky's (1933) The Redshift of Extragalactic Nebulae. *ArXiv e-prints*, November 2017.

[6] M. Schwarzschild. Mass distribution and mass-luminosity ratio in galaxies. 59:273, September 1954.

[7] Meekins J. F., Fritz G., Chubb T. A., and Friedman H. Physical Sciences: X-rays from the Coma Cluster of Galaxies. 231:107–108, May 1971.

[8] A. Penzias. Free Hydrogen in the Pegasus I Cluster of Galaxies. 66:293, March 1961.

[9] D. H. Rogstad and G. S. Shostak. Gross Properties of Five Scd Galaxies as Determined from 21-CENTIMETER Observations. 176:315, September 1972.

[10] M. S. Roberts and R. N. Whitehurst. The rotation curve and geometry of M31 at large galactocentric distances. 201:327–346, October 1975.

[11] V. C. Rubin and W. K. Ford, Jr. Rotation of the Andromeda Nebula from a Spectroscopic Survey of Emission Regions. 159:379, February 1970.

[12] J. P. Ostriker, P. J. E. Peebles, and A. Yahil. The size and mass of galaxies, and the mass of the universe. 193:L1–L4, October 1974.

[13] J. F. Navarro, C. S. Frenk, and S. D. M. White. The Structure of Cold Dark Matter Halos. 462:563, May 1996.

[14] Mariangela Lisanti. Lectures on Dark Matter Physics. In *Proceedings, Theoretical Advanced Study Institute in Elementary Particle Physics: New Frontiers in Fields and Strings (TASI 2015): Boulder, CO, USA, June 1-26, 2015*, pages 399–446, 2017.

[15] John S. Gallagher III Linda S. Sparke. *Galaxies in the Universe: An Introduction*. Cambridge University Press, 2 edition, 2007.

[16] Sebastián Franco Ulloa. Simulaciones de un fluido débilmente auto-interactuante con métodos de lattice-boltzmann. Master's thesis, Universidad de los Andes, 5 2017.

[17] Philip Mocz and Sauro Succi. Integer lattice dynamics for Vlasov–Poisson. *Mon. Not. Roy. Astron. Soc.*, 465(3):3154–3162, 2017.

[18] V. Fuka. PoisFFT - A Free Parallel Fast Poisson Solver. *ArXiv e-prints*, September 2014.

[19] J.W Eastwood R.W Hockney. *Computer simulation using particles.*

[20] Matteo Frigo and Steven G. Johnson. The design and implementation of FFTW3. *Proceedings of the IEEE*, 93(2):216–231, 2005. Special issue on "Program Generation, Optimization, and Platform Adaptation".

[21] F. Nesti and P. Salucci. The Dark Matter halo of the Milky Way, AD 2013. 7:016, July 2013.

[22] Prieto Asinari. *Multi-Scale Analysis of Heat and Mass Transfer in Mini/Micro-Structures.* PhD thesis, Politecnico di Torino, 2005.

[23] P. A. R. Ade et al. Planck 2013 results. I. Overview of products and scientific results. *Astron. Astrophys.*, 571:A1, 2014.

[24] P. Gondolo and G. Gelmini. Cosmic abundances of stable particles: improved analysis. *Nuclear Physics B*, 360:145–179, August 1991.

[25] Dr Jian Guo Zhou. *Lattice Boltzmann Method.* 01 2004.

[26] Andrew Liddle. *An Introduction to Modern Cosmology*. Wiley, 2nd ed edition, 2003.

[27] Aleksei Parnowski Serge Parnovsky. *How the Universe Works: Introduction to Modern Cosmology*. World Scientific Publishing, 2018.

[28] M. Xiaochun, X. Kuan, and Y. Ping. The Calculations of Gravity Fields and Rotation Curves of Whirlpool Galaxies and Dark Material. *ArXiv e-prints*, March 2009.

[29] Frederick Reif. *Fundamentals of statistical and thermal physics*. McGraw-Hill Series in Fundamentals of Physics. McGraw-Hill Science/Engineering/Math, 1 edition, 1965.

[30] Ostlie D.A. Carroll B.W. *An introduction to modern astrophysics*. 2ed., pearson edition, 2007.